Energy calibration of data recorded with the surface detectors of the Pierre Auger Observatory

Claudio Di Giulio*, for the Pierre Auger Collaboration†

*Università and INFN di Roma II, "Tor Vergata", Via della Ricerca Scientifica 1,00133 Roma, Italy
†Observatorio Pierre Auger, Av. San Martin Norte 304, 5613 Malargüe, Argentinia

***Abstract*. The energy of the primary particles of air showers recorded using the water-Cherenkov detectors of the Pierre Auger Observatory is inferred from simultaneous measurements of showers together with the fluorescence telescopes. The signal on the ground at 1000 m from the shower axis obtained using the water-Cherenkov detectors is related directly to the calorimetric energy measured with the telescopes. The energy assignment is therefore independent of air-shower simulations except for the assumptions that must be made about the energy carried into the ground by neutrinos and muons. The correlation between the signal at ground and the calorimetric energy is used to derive a calibration curve. A detailed description of the method used to determine the energy scale is presented. The systematic uncertainties on the calibration procedure are discussed.**

***Keywords*: UHECR, energy spectrum, Auger, Calibration.**

I. Introduction

The Pierre Auger Observatory [1] detects air showers with over 1600 water-Cherenkov detectors, collectively called the surface detector (SD). The SD measures the lateral distribution of particles in air showers with a duty cycle of almost 100% [2]. The SD is overlooked by the fluorescence detector (FD) which consists of 24 fluorescence telescopes grouped in units of 6 at four locations on the periphery of the SD. The FD is only used on clear moonless nights, and has a duty cycle of 13% [3]. The FD provides a nearly calorimetric energy measurement, $E_{\rm FD}$, since the fluorescence light is produced in proportion to the energy dissipation by a shower in the atmosphere [4], [5]. An example of a reconstruction of a typical air shower with an energy of $40\,\mathrm{EeV}$ and a zenith angle of 36° detected with the SD and FD is shown in figures 1 and 2.

The signals recorded in a water-Cherenkov detector are converted in terms of vertical equivalent muons (VEM). One VEM represents the average of the signals produced in the 3 PMTs of the detector by a vertical muon that passes centrally through the SD detector unit. The air shower axis is obtained from the arrival time of the first particles in each detector station. The impact point on ground and the lateral distribution of signals are obtained in a global maximum likelihood minimization which accounts for the station trigger threshold and the overflow of the FADCs counts in the stations very close to the shower axis. The effect of the fluctuation of the lateral distribution function is minimized at $1000\,\mathrm{m}$.

The interpolated signal at a fixed distance from the shower core correlates well with the energy of the primary cosmic ray [6]. The signal at distance of $1000\,\mathrm{m}$, S(1000), indicated as a cross in figure 1 is used as energy estimator.

For the air showers that are also observed with the fluorescence telescopes a direct measurement of the longitudinal profile of the air shower is possible. The longitudinal profile of the air shower, i.e. the energy deposit as a function of traversed matter in the atmosphere, is obtained determining first the shower geometry and then accounting for the fluorescence and Cherenkov light contributions and the light scattering and attenuation [7]. The shower axis is derived using the timing information and the direction of the triggered PMTs of the fluorescence telescope and using the timing information of the water-Cherenkov detector with the highest signal, this allow an angular resolution better than 1°. The FADCs counts recorded by the PMTs of the fluorescence telescope are converted into photons using the calibration constant derived night by night [8]. The timing information is converted in atmospheric slant depth correcting for the measured atmospheric condition [9]. From the estimated fluorescence light the energy deposit profile is obtained using the absolute fluorescence yield in air which at $293\,\mathrm{K}$ and $1013\,\mathrm{hPa}$ at $337\,\mathrm{nm}$ band is 5.05 ± 0.71 photons$/\mathrm{MeV}$ of energy deposited [10]. The fluorescence yield pressure and wavelength dependency are accounted for [11].

Due to the limited field of view, the longitudinal profile is not entirely recorded, so a fit with a Gaisser-Hillas function is employed to obtain the full profile.

The subsample of air showers that are recorded by both detectors, called "hybrid events", are used to relate $E_{\rm FD}$ to $S(1000)$. The energy scale inferred from this data sample is applied to the full sample of showers detected by the array of the water-Cherenkov detectors.

II. Data Analysis

A subset of high-quality hybrid events detected between January 2004 and December 2008 with reconstructed zenith angle less than 60° are used in this analysis [12]. To ensure that a shower recorded by the SD has a reliable estimate of $S(1000)$, accidental

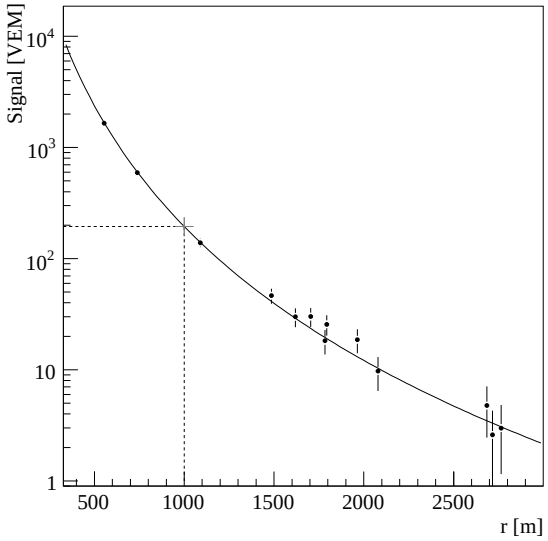

Fig. 1. Lateral distribution: filled circles represent recorded signals. The fitted value S(1000) is marked with a cross.

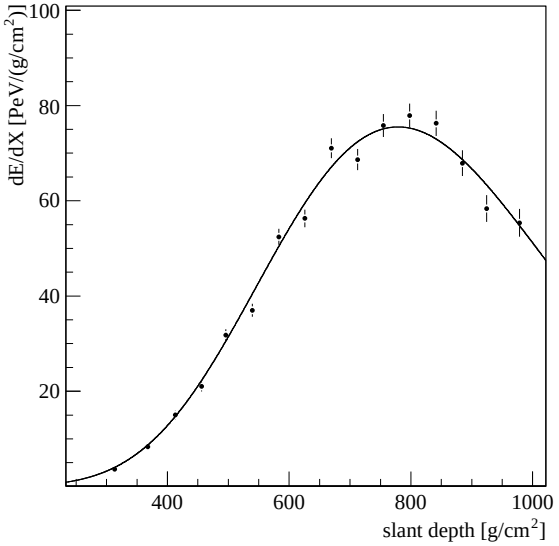

Fig. 2. Longitudinal profile: energy deposit in the atmosphere as a function of the slant depth.

triggers are rejected and all six nearest neighbours of the station with the largest signal must be active. This guarantees the core of the shower being contained within the array. The geometry of an event is determined from the times recorded at a fluorescence telescope, supplemented by the time of the water-Cherenkov detector with the highest signal. This station must be within $750\,\mathrm{m}$ from the shower axis [13]. The reduced χ^2 of the longitudinal profile fit to the Gaisser-Hillas function [7] has to be less than 2.5. Events are rejected by requiring that the χ^2 of a linear fit to the longitudinal profile exceeds the Gaisser-Hillas fit χ^2 by at least four. The depth of shower maximum, X_{max}, has to be within the field of view of the telescopes and the fraction of the signal detected by the fluorescence telescopes and attributed to Cherenkov light must be less than 50%. The uncertainties on E_{FD} being lower than 20% and on X_{max} lower than $40\,\mathrm{g/cm^2}$ are also requested. The selection criteria include a measurement of the vertical aerosol optical depth profile (VAOD(h)) [14] using laser shots generated by the central laser facility (CLF) [15] and observed by the fluorescence telescopes in the same hour of each selected hybrid event. For a given energy the value of $S(1000)$ decreases with zenith angle, θ, due to the attenuation of the shower particles and geometrical effects. Assuming an isotropic flux for the whole energy range considered, we extract the shape of the attenuation curve from the data [16]. The fitted attenuation curve, $CIC(\theta) = 1 + a\ x + b\ x^2$, is a quadratic function of $x = \cos^2\theta - \cos^2 38^\circ$ and is displayed in figure 3 for a particular constant intensity cut which corresponds to $S_{38^\circ} = 47\,\mathrm{VEM}$, with $a = 0.90 \pm 0.05$ and $b = -1.26 \pm 0.21$. The average angle is $\langle\theta\rangle \simeq 38^\circ$ and we take this angle as reference to convert $S(1000)$ into S_{38° by $S_{38^\circ} \equiv S(1000)/CIC(\theta)$. It may be regarded as the signal $S(1000)$ the shower would have produced had it arrived at $\theta = 38^\circ$.

The reconstruction accuracy $\sigma_{S(1000)}$ of the parameter $S(1000)$ is composed by 3 contributions: a statistical uncertainty due to the finite size of the detector and the limited dynamic range of the signal detection, a systematic uncertainty due to the assumptions of the shape of the lateral distribution and finally due to the shower-to-shower fluctuations [17]. The relative uncertainty is shown in figure 4, and in the range of interest, $\sigma_{S_{38^\circ}}/S_{38^\circ} \simeq 14\%$.

Not all the energy of a primary cosmic ray particle ends up in the electromagnetic part of an air shower detected by fluorescence telescopes. Neutrinos escape undetected and muons need long path lengths to release their energy. This non-detected energy is sometimes called the *invisible energy*, and is usually accounted for

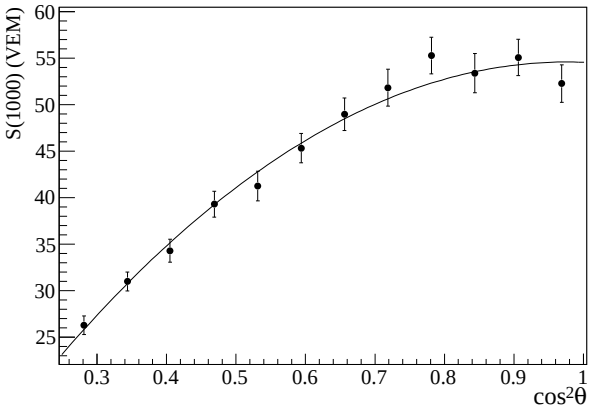

Fig. 3. Derived attenuation curve, $CIC(\theta)$, fitted with a quadratic function.

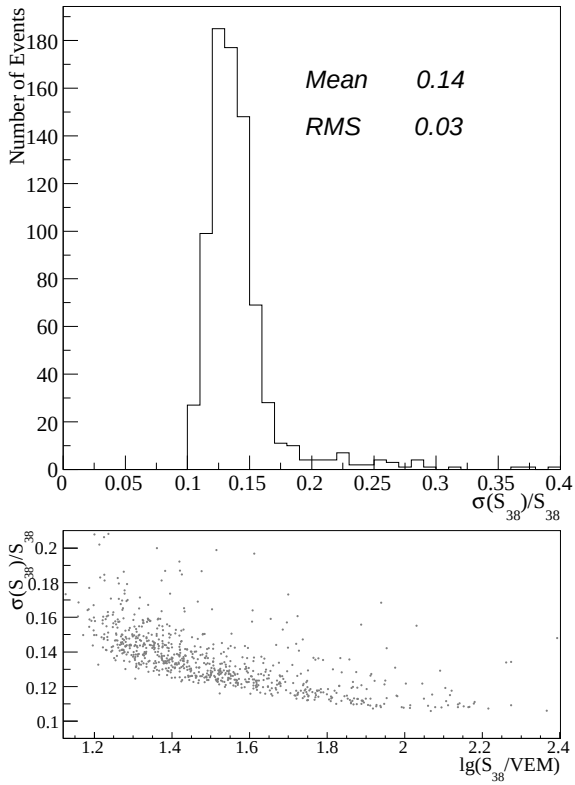

Fig. 4. Upper panel: S_{38° resolution. Lower panel $\sigma_{S_{38^\circ}}/S_{38^\circ}$ on function of $lg(S_{38^\circ}/VEM)$ scatter plot.

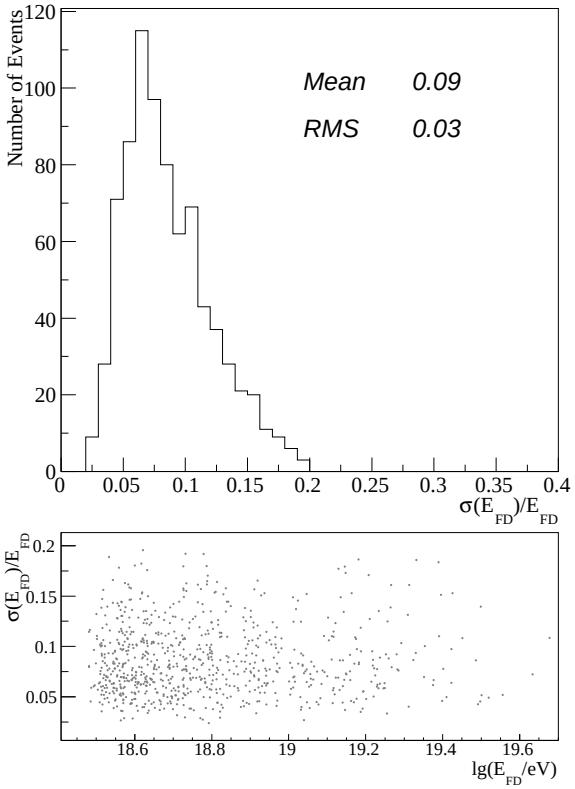

Fig. 5. Upper panel: $E_{\rm FD}$ resolution. Lower panel $\sigma_{E_{\rm FD}}/E_{\rm FD}$ on function of $lg(E_{\rm FD}/eV)$ scatter plot.

by correcting the electromagnetic energy $E_{\rm em}$, detected by fluorescence telescopes. The factor f_{inv} is determined from shower simulations to obtain the total shower energy $E_{\rm FD} = f_{inv}\, E_{\rm em}$. The *invisible energy* correction is based on the average for proton and iron showers simulated with the QGSJet model and sums up to about 10% at 10 EeV. The neutrino and muon production probabilities have energy dependencies due to the meson decay probabilities in the atmosphere. Thus, the factor f_{inv} depends on the energy for different hadronic interaction models and is also subject to shower-to-shower fluctuations [18].

The statistical uncertainties, $\sigma_{E_{\rm FD}}$, of the total energy, $E_{\rm FD}$, measured by the fluorescence telescopes is composed of the statistical uncertainty of the light flux, σ_{flux}, the uncertainty due to the core location and shower direction, σ_{geo}, the uncertainty on the invisible energy correction, σ_{inv} and the uncertainty related to the measured VAOD profile, σ_{atm}. The total relative uncertainty is about $\sigma_{E_{\rm FD}}/E_{\rm FD} = 9\%$ as shown in figure 5 and does not depend strongly on the energy.

III. Calibration Curve

The relation of S_{38} and $E_{\rm FD}$ for the 795 hybrid selected events in the energy region where the surface detector array is fully efficient, $E \geq 3$ EeV, is well described by a power-law function,

$$E = a\ S_{38}^{b}, \tag{1}$$

as shown in figure 6. The results of a fit to the data are

$$a = (1.51 \pm 0.06(stat) \pm 0.12(syst)) \times 10^{17}\,\text{eV},$$
$$b = 1.07 \pm 0.01(stat) \pm 0.04(syst),$$

with a reduced χ^2 of 1.01. S_{38} grows approximately linearly with energy. The root-mean-square deviation of the distribution is about 17% as shown in figure 7, in good agreement with the quadratic sum of the statistical uncertainties of S_{38° and $E_{\rm FD}$. The calibration accuracy at the highest energies is limited by the number of recorded showers: the most energetic selected event is about $6 \times 10^{19}\,\text{eV}$. The calibration at low energies extends below the range of interest.

IV. Systematic Uncertainties

The systematic uncertainty due to the calibration procedure is 7% at $10^{19}\,\text{eV}$ and 15% at $10^{20}\,\text{eV}$.

The systematic uncertainties on the energy scale $E_{\rm FD}$ sum up to 22%. The largest uncertainties are given by the absolute fluorescence yield (14%) [10], the absolute calibration of the fluorescence telescopes (9%) and the uncertainty due to the reconstruction method of the longitudinal shower profile (10%).

The uncertainty due to the water vapour quenching on the fluorescence yield (5%) is taken into account as

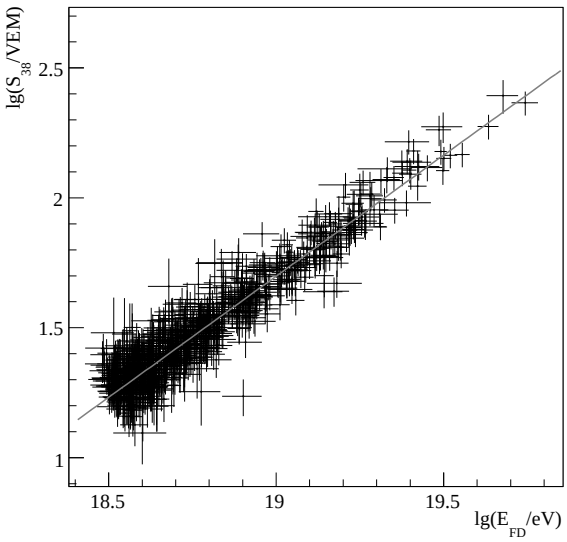

Fig. 6. Correlation between $\lg S_{38}$ and $\lg E_{\rm FD}$ for the 795 hybrid events used in the fit. The line represents the best fit.

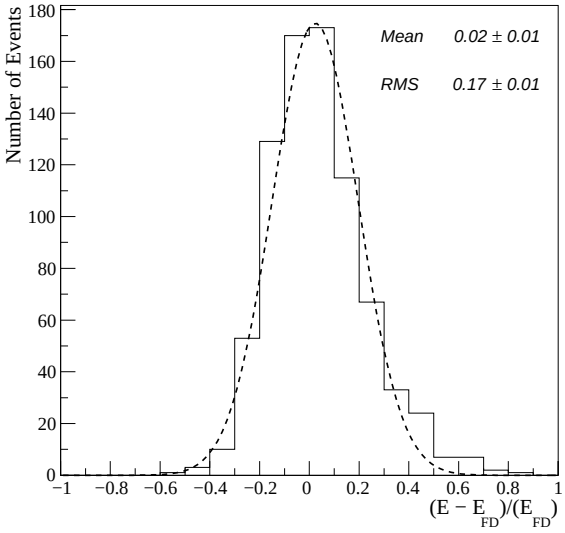

Fig. 7. Fractional difference between the calorimetric energy, $E_{\rm FD}$, and the energy estimate of the surface detector, E, obtained by the calibration curve, for the 795 selected events.

described in [19]. Additionally, the wavelength dependent response of the fluorescence telescopes (3%), the uncertainties on measurements of the molecular optical depth (1%), on the measurements of the aerosol optical depth (7%) and on multiple scattering models (1%) are included in the overall systematic uncertainty. The *invisible energy* correction contributes 4% to the total systematic uncertainty of 22% [20].

V. Outlook

The energy calibration of the surface detector array was obtained with measurements of the fluorescence telescopes and a detailed study of the uncertainties was given. Several activities are on-going to reduce the systematic uncertainties of the energy estimate, e.g. the longitudinal profile reconstruction method and the uncertainty of the fluorescence yield. The spectrum derived from data of the surface detector array is calibrated using the method presented in this paper and compared with a spectrum based on measured hybrid data in [21].

References

[1] J. Abraham [Pierre Auger Collaboration], NIM 523 (2004) 50.
[2] T. Suomijarvi [Pierre Auger Collaboration] Proc. 30^{th} ICRC, Merida, (2007), **4**, 311.
[3] F. Salamida [Pierre Auger Collaboration] these proceedings, (2009) #0109.
[4] M. Risse and D. Heck, Astropart. Phys. 20 (2004) 661.
[5] H. Barbosa et al., Astropart. Phys. 22 (2004) 159.
[6] A. M. Hillas, Acta Physica Academiae Scientiarum Hungaricae Suppl. 3 **29** (1970), 355.
[7] M. Unger *et al.*, Nucl. Instr. and Meth. **A 588**, 433 (2008).
[8] R. Caruso [Pierre Auger Collaboration] these proceedings, (2009) #0358.
[9] L. Valore [Pierre Auger Collaboration] these proceedings, (2009) #0087.
[10] M. Nagano, K. Kobayakawa, N. Sakaki, K. Ando, Astropart. Phys. 22 (2004) 235.
[11] M. Ave *et al.* Astropart. Phys. 28 (2007) 41.
[12] D. Allard [Pierre Auger Collaboration], Proc. 29^{th} ICRC, Pune (2005), **7**, 71.
[13] L. Perrone [Pierre Auger Collaboration] Proc. 30^{th} ICRC, Merida, (2007), **4**, 331.
[14] S. Ben-Zvi [Pierre Auger Collaboration] Proc. 30^{th} ICRC, Merida, (2007), **4**, 355.
[15] B. Fick et al., JINST, 1 (2006) 11003.
[16] J. Hersil et al. Phys. Rev. Lett. **6**, 22 (1961).
[17] M. Ave [Pierre Auger Collaboration] Proc. 30^{th} ICRC, Merida, (2007), **4**, 307.
[18] T. Pierog et al., Proc. 29^{th} ICRC, Pune (2005).
[19] S. Ben-Zvi [Pierre Auger Collaboration] these proceedings, (2009) #0083.
[20] B. Dawson [Pierre Auger Collaboration] Proc. 30^{th} ICRC, Merida, (2007), **4**, 425.
[21] F. Schüssler [Pierre Auger Collaboration] these proceedings, (2009) #0114.